

Limits to multipartite entanglement generation with bosons and fermions

Malte C. Tichy,^{1,2} Florian Mintert,^{3,1} and Andreas Buchleitner¹

¹*Physikalisches Institut, Albert-Ludwigs-Universität Freiburg,
Hermann-Herder-Strasse 3, D-79104 Freiburg, Germany*

²*Lundbeck Foundation Theoretical Center for Quantum System Research,*

Department of Physics and Astronomy, University of Aarhus, DK-8000 Aarhus C, Denmark

³*Freiburg Institute for Advanced Studies, Albert-Ludwigs-Universität, Albertstrasse 19, 79104 Freiburg, Germany*

(Dated: October 14, 2012)

Many-photon interference in linear-optics setups can be exploited to generate and detect multipartite entanglement. Without recurring to any inter-particle interaction, many entangled states have been created experimentally, and a panoply of theoretical schemes for the generation of various classes of entangled states is available. Here, we present a unifying framework that accommodates the present experiments and theoretical protocols for the creation of multiparticle entanglement via interference. A general representation of the states that can be created is provided for bosons and fermions, for any particle number, and for any dimensionality of the entangled degree of freedom. Using the framework, we derive an upper bound on the generalized Schmidt number of the states that can be generated, and we establish bounds on the dimensionality of the manifold of these states. We show that – at the expense of a smaller success probability – more states can be created with bosons than with fermions, and give an intuitive interpretation of the state representation and of the established bounds in terms of superimposed many-particle paths.

I. INTRODUCTION

The preparation of entangled states of photons [1] has been the subject of a great collective effort, which was driven by fundamental scientific questions such as the violation of local realism [2–4] as well as by the perspective of technological applications, including, *e.g.*, quantum cryptography [5] and quantum computing [6]. The control over the process of spontaneous parametric down-conversion (SPDC) started this successful journey in 1988, when a two-photon entangled state was created [7]. This achievement was followed, in 1999, by the creation of an entangled tripartite state [8]. Step-by-step-wise, the number of photons was further increased, such that entanglement in four-photon [9], five-photon [10], six-photon [11–14], and, eventually, eight-photon states [15, 16] was demonstrated. While many experiments can generate only one particular state, there are also setups that can tune the final state through several classes of qualitatively different types of multipartite entanglement [17] by varying parameters in the scattering setup [18].

The creation of an entangled state of photons relies on the independent propagation of the particles in a linear-optics setup and on the subsequent selection of successful final states with one particle in each spatial output mode, *i.e.* on *post-selection*. No direct interaction between the photons takes place, in contrast to other possible carriers of entanglement such as trapped ions [19]. It is, in contrast, the *indistinguishability* of the photons which provides the seed for quantum correlations. Therefore, the physical mechanism – the coherent superposition of many-particle paths – is rather independent of the practical experimental implementation. For example, also the indistinguishability of cold atoms can be used for interaction-free entanglement generation [20].

Whereas in the mentioned examples for multiphoton

entanglement, quantum correlations are encoded in the polarization of the photons, also other degrees of freedom can be used to carry entanglement, such as the time-bin [21–23], the path [7, 24], or the orbital angular momentum [25–28]. Since degrees of freedom other than polarization are not restricted to two dimensions, their use renders the creation and detection of entanglement in higher dimensions possible. In particular, genuine qutrit-entanglement was realized with energy-time entangled photons [29], and the encoding of a 20-dimensional degree of freedom in the time-bin of was demonstrated with a single photon [30].

Besides the variety of entangled states that has been created experimentally with photons by now [1, 13, 14, 18, 31], manifold further strategies for the creation of large classes of entangled states were proposed [32–38]; but although all these schemes share the same physical ingredients, no common framework permits the direct comparison of these approaches. With the rapidly increasing complexity of many-particle interference setups with growing particle number, a general framework is highly desirable for the design of setups with high success rate and low number of components, and for the systematic comparison of competing approaches to multipartite entanglement generation [37, 38]. A common language for a unified description of such existing schemes, and for possible new strategies is our first desideratum in this article.

From the conceptual perspective, we also lack an understanding for the intrinsic limitations of setups that rely on many-particle interference. At first sight, it seems that a very large set of entangled states of photons of nearly arbitrary particle number and dimension can be created in the laboratory. It was, however, also recognized that a toolbox composed of linear optics and post-selection alone is by far not universal, *i.e.* a setup that

relies uniquely on the indistinguishability of particles imposes severe restrictions on the implementable quantum operations. Consequently, several no-go theorems were formulated for few-particle systems. For example, a Bell measurement that can discriminate all four Bell-states is impossible with linear optics [39]. Similarly, teleportation with 100% success cannot be achieved using photons [40]. On the other hand, the manipulation and characterization of qudits, *i.e.* higher-dimensional degrees of freedom, is severely constrained: The Schmidt-rank of any measurement operator on two qubits is bound by N , when $N - 2$ auxiliary qudits are available [41].

While the characterization and the classification of general multipartite entangled states is rapidly progressing [42–47], it becomes desirable to understand the general physical principles that limit the creation of multipartite qudit-like entangled states. Also for this enterprise, a common framework that describes generic many-particle interference-based setups is a mandatory requirement. Such framework should, both, describe the physical processes that lead to a certain final state, and offer a representation of this state that permits an investigation with the tools of quantum information theory, like entanglement measures. In other words, such framework should bridge the gap between the *physical* many-particle scattering process and the *abstract* quantum state of quantum information theory.

Here, we set the stage for a systematic investigation of the aforementioned problems. We propose a treatment of general entanglement-generating setups which accommodates virtually all possible schemes that use identical particles, where the particles carry (typically internal) degrees of freedom that may or may not be entangled. Thereby, all existing schemes for photons can be understood in equal terms: The created state emerges as a coherent superposition of many-particle paths [48], which can be traced back to the state representation. This state representation allows us to investigate systematically the capabilities of interference-based setups and to characterize the set of states that can be created, with the tools of quantum information theory. In particular, we find a general combinatorial bound for the maximal generalized Schmidt number [49] for multipartite entangled states of qudits, which generalizes a previously known theorem for two particles [41]. This bound constitutes an intuitive restriction of the set of states that can be generated, and a physical characterization of the intrinsic limitations of interference-based entanglement generation. It applies equally for bosons and fermions, for which, however, the dimensionality of the set of states that can be created is different, as we will also show. As a consequence, more states can be generated with bosons than with fermions, at the expense of a lower success probability of entanglement generation for bosons.

We first establish the general experimental capabilities that are available today, and those which may become available in the near future, in Section II. On that basis, we formulate the requirements that a versatile model

should fulfill, and develop a framework that satisfies these demands. An explicit representation of the achievable multipartite states is then derived in Section III, which allows the formulation of a general bound on the Schmidt number of the generated states. We then show in Section IV that this bound is not the only restriction that applies to interference-based setups, since the number of dimensions of the manifold of states that can be created with bosons and fermions establishes another limitation, with a tighter bound for fermions than for bosons. Concluding discussions are given in Section V. For illustration, and in order to familiarize the reader with the methods and with our framework, we schematically reproduce several state-of-the-art experiments and theoretical schemes in Appendix A. The derivation of the dimensional bounds is presented in Appendix B.

II. UNIFIED FRAMEWORK FOR ENTANGLEMENT GENERATION

A. Physical situation and versatility requirements

The examples for entanglement generation that were mentioned in the introduction are all based on the same principle mode of operation: Several photons prepared in a given initial state propagate through a linear-optics setup. Post-selection is performed on events at the output modes, and only events with exactly one particle in each spatial mode are taken into account. Given such a post-selected, successful event, the internal states of the particles have then the desired entanglement properties. While photons are destroyed in the moment they are detected in an optical mode, the presence of massive particles in a target mode can be ensured by some measurement that leaves the particle and the entangled degree of freedom it carries unaffected, and the entangled particles may be used for further processing. Besides entanglement generation via propagation and post-selection, also the projection onto entangled states and the detection of entangled states is possible with techniques that are based on the same principles [18, 50].

Given the rather broad variety of existing schemes and successful experiments, our dedicated attempt to formalize the state-of-the-art under one housetop should fulfill the following requirements:

- Any number of particles N is allowed.
- Entanglement is established between arbitrary d -dimensional degrees of freedom.
- The coherent manipulation of the entangled degrees of freedom is possible without restriction.
- The initial state may or may not be entangled.
- Bosons as well as fermions may carry the entanglement.

- The creation of entanglement as well as the projection onto entangled states are contained in the description.

In contrast to the polarization of photons, which can be manipulated essentially without restrictions, it is not immediate that all coherent single-particle operations or state-dependent beamsplitters can be implemented for any other degree of freedom [51]. Depending on the chosen physical carrier of entanglement – *e.g.* polarization, time-bin, path, or orbital angular momentum –, it may be possible that, *e.g.*, operations that discriminate the internal degrees of freedom are difficult to implement [51, 52]. It is therefore important to pay particular attention to the modeling of different types of setups with distinct capabilities, as we will do in Section II E.

B. Many-particle states and their interpretation

A central building block of our present approach is the description of the physical many-particle scattering process and its relationship to the entangled states it generates. We emphasize the conceptual difference between the abstract, quantum-information interpretation of a state (the “ N -qudit-state”), and its *physical realization*, which we will need to work with in parallel.

For the understanding of an experiment, it is useful to describe *physical states* of photons or other identical particles in second quantization; we will denote these states by $|\Psi^{2q}\rangle$. In this representation, we can formulate the physical many-particle scattering process, whereas the definition of an entanglement content requires the identification of a subsystem structure which is most adequately done in first quantization [53]. Within a clear tensor structure that is imposed by physical observables, the usual means to characterize entanglement, such as monotones and measures [54], can then be applied on the first-quantized state $|\Phi^{1q}\rangle$.

Since the dynamics is best described in second quantization, whereas first quantization is more appropriate for the description of entanglement properties, we will specify a map, $\hat{\Omega}_a$, between both representations such that $|\Psi^{2q}\rangle = \hat{\Omega}_a |\Phi^{1q}\rangle$. We emphasize that the conceptual problem of the assignment of entanglement to a state of identical particles [55–57] is circumvented by the present treatment, since states of identical particles $|\Psi^{2q}\rangle$ are identified with states of distinguishable subsystem components $|\Phi^{1q}\rangle$. Before we can define this map, let us briefly review the essential properties of quantum states.

1. State representation

An N -qudit-state,

$$|\Phi^{1q}(c)\rangle = \sum_{j_1=1}^d \cdots \sum_{j_N=1}^d c_{j_1, \dots, j_N} |j_1, \dots, j_N\rangle, \quad (1)$$

is fully specified by the d^N components of the coefficient tensor

$$c \in \mathbb{C}^d \otimes \mathbb{C}^d \otimes \cdots \otimes \mathbb{C}^d. \quad (2)$$

The subsystem structure in (1) and (2) reflects the paradigmatic situation of N parties that each control a d -dimensional subspace. Therefore, the usual notions of separability and entanglement can be applied on $|\Phi^{1q}(c)\rangle$ [17, 58, 59]. For instance, the state $|\Phi^{1q}(c)\rangle$ is fully separable (or N -separable) if c_{j_1, \dots, j_N} can be written as a product,

$$c_{j_1, \dots, j_N} = c_{j_1}^{(1)} \cdot c_{j_2}^{(2)} \cdot \cdots \cdot c_{j_N}^{(N)}. \quad (3)$$

The N -qudit-state $|\Phi^{1q}(c)\rangle$ is realized in the experiment as a physical state $|\Psi^{2q}(c)\rangle$ of N bosons or fermions that each carry a d -dimensional degree of freedom. Since the carriers of entanglement are indistinguishable particles, each subsystem is of the same dimension d . This degree of freedom will typically be an internal property of the particle, such as polarization or orbital angular momentum. In the following, we will always refer to entanglement between these internal degrees of freedom when speaking of entanglement between particles. Additionally, the particles are distinguished by some external, discriminating degree of freedom – typically the spatial mode. Our description thus requires N spatial modes (as many as particles), such that the minimal size of the single-particle Hilbert space for a description in second quantization has dimension $n = d \cdot N$, since each particle can live in any of the N modes, due to indistinguishability. In order to incorporate setups that treat different internal degrees of freedom in a distinct way (the internal state of an incoming particle may change during the scattering process), we choose a notation in which the internal (entangled) and external (discriminating) degrees of freedom are not explicitly distinguished, which will considerably simplify the subsequent discussion. For this purpose, the first d physical modes (of a total of n modes) are interpreted as the d internal states of a particle that is prepared in the first spatial mode, the second d modes represent the d internal states of a particle in the second spatial mode, and so on. In other words, we consider the entanglement between the particles found in groups of d modes.

The creation operator $\hat{a}_{k,l}^\dagger$ creates a particle in the k th spatial mode and in the l th internal state, and we identify

$$\hat{a}_{k,l}^\dagger \equiv \hat{a}_{d(k-1)+l}^\dagger. \quad (4)$$

With this convention, a second-quantized state possesses an interpretation in terms of N (first quantized) particles that are controlled by N parties – the usual quantum information paradigm of an N -qudit-state – only if there is exactly one particle per group of d modes. We call such physical states that can be interpreted as N -qudit-state *post-selected states*, since these are precisely the states that are obtained by post-selection. Any N -qudit-state in first quantization possesses a representation in second quantization, but not vice-versa.

The second-quantized version of the initial N -qudit-state $|\Phi^{1q}(c)\rangle$ in (1) is thus necessarily a post-selected state,

$$|\Psi^{2q}(c)\rangle = \sum_{j_1=1}^d \cdots \sum_{j_N=1}^d c_{j_1, \dots, j_N} \prod_{k=1}^N \hat{a}_{d \cdot (k-1) + j_k}^\dagger |\text{vac}\rangle, \quad (5)$$

where $|\text{vac}\rangle$ denotes the vacuum. The occupation of the $n = d \cdot N$ physical modes is characterized by a *mode occupation list*,

$$\vec{r} = (r_1, r_2, \dots, r_n), \quad (6)$$

which describes a state with r_j particles in the j th mode. Equivalently, we can specify the modes in which the N particles are located, *i.e.* define a *mode assignment list*. For the state (5), the latter reads

$$\vec{d}(\vec{r}) = (j_1, d + j_2, 2d + j_3, \dots, (N-1)d + j_N). \quad (7)$$

We illustrate the mode occupation and mode assignment lists of several distinct physical states and the corresponding N -qudit-states in Table I.

d	N	occupation \vec{r}	assignment $\vec{d}(\vec{r})$	$ \Phi^{1q}\rangle$
3	2	$(\underbrace{1, 0, 0}, \underbrace{0, 1, 0})$	(1,5)	$ 1, 2\rangle$
2	3	$(\underbrace{1, 0}, \underbrace{1, 0}, \underbrace{0, 1})$	(1,3,6)	$ 1, 1, 2\rangle$
2	4	$(\underbrace{1, 0}, \underbrace{0, 1}, \underbrace{0, 1}, \underbrace{1, 0})$	(1,4,6,7)	$ 1, 2, 2, 1\rangle$
2	3	$(\underbrace{1, 0}, \underbrace{1, 1}, \underbrace{0, 0})$	(1,3,4)	no
3	2	$(\underbrace{1, 0, 1}, \underbrace{0, 0, 0})$	(1,3)	no
2	2	$(\underbrace{2, 0}, \underbrace{0, 0})$	(1,1)	no

TABLE I: **Physical Fock states and interpretation as N -qudit-states** $|\Phi^{1q}\rangle$. The Fock states are defined by the mode occupation list \vec{r} , Eq. (6), or, equivalently, by the mode assignment list $\vec{d}(\vec{r})$, Eq. (7). If exactly one particle is present in each group of d modes (which are emphasized by the brackets), there is a corresponding first-quantized N -qudit-state $|\Phi^{1q}\rangle$. The last three states correspond to unsuccessful scattering events and cannot be used for quantum-information purposes within our scheme.

2. Map

As anticipated above, we define an explicit map $\hat{\Omega}_a$ between the first-quantized N -qudit-state and the second-quantized representation,

$$\hat{\Omega}_a = \sum_{j_1=1}^d \cdots \sum_{j_N=1}^d \left[\prod_{k=1}^N \hat{a}_{j_k + (k-1)d}^\dagger \right] |\text{vac}\rangle \langle j_1, \dots, j_N |^{1q}, \quad (8)$$

such that

$$\begin{aligned} |\Psi^{2q}(c)\rangle &= \hat{\Omega}_a |\Phi^{1q}(c)\rangle, \\ |\Phi^{1q}(c)\rangle &= \hat{\Omega}_a^\dagger |\Psi^{2q}(c)\rangle = \hat{\Omega}_a^{-1} |\Psi^{2q}(c)\rangle. \end{aligned} \quad (9)$$

The map $\hat{\Omega}_a$ is defined for a given particle-number N , and invertible only for the subset of post-selected many-particle states. The post-selection procedure is described by the projector $\hat{P}_{1,a}$ on the subspace of states with exactly one particle in each group of d modes,

$$\hat{P}_{1,a} = \sum_{j_1, \dots, j_N=1}^d \left(\prod_{k=N}^1 \hat{a}_{d(k-1)+j_k}^\dagger \right) \left(\prod_{k=1}^N \hat{a}_{d(k-1)+j_k} \right) \quad (10)$$

where the inverted order of the indices for the creation operators avoids sign changes due to the exchange of fermions. For example, the first three states given in Table I are eigenstates of $\hat{P}_{1,a}$ and possess an interpretation as N -qudit-state, whereas the last three do not and lie in the kernel of $\hat{P}_{1,a}$.

C. Many-particle evolution

The manipulation of entanglement by the thus defined setup relies on the scattering of non-interacting particles that carry the possibly entangled internal degree of freedom. In other words, the time-evolution of a physical initial state $|\Psi^{2q}(c)\rangle = \hat{\Omega}_a |\Phi^{1q}(c)\rangle$ is governed by a single-particle scattering matrix W that connects n input modes \hat{a}_j^\dagger to n output modes \hat{b}_k^\dagger . The state of each particle prepared in an input mode thus evolves into a superposition of amplitudes localized at different output modes:

$$\hat{a}_j^\dagger \rightarrow \sum_{k=1}^n W_{j,k} \hat{b}_k^\dagger. \quad (11)$$

The physical scattering process is governed by the Schrödinger equation, it is thus unitary. The scattering matrix W , however, is non-unitary, in general, since particle loss may occur, *i.e.* a particle that is prepared in an input mode has a finite amplitude to not reach any output mode. The matrix W is, in general, embedded in a unitary matrix of dimension $(2n-1) \times (2n-1)$ [60, 61], such that

$$U = \begin{pmatrix} W & X \\ Y & Z \end{pmatrix}, \quad (12)$$

where X, Y, Z are matrices of dimension $n \times (n-1)$, $(n-1) \times n$ and $(n-1) \times (n-1)$, respectively, *i.e.* at least $n-1$ auxiliary modes are needed to account for particle loss. The non-vanishing matrix elements of X describe the loss of particles, *i.e.* they quantify the transition amplitudes that describe the processes in which an injected particle is not collected by any of the first n modes. For example, particles may be lost in free-space propagation schemes [33, 34, 62]. The embedding matrix U can be inverted, and the inverse scattering process on the n modes of interest (with the input and output modes exchanged) is thus described by W^\dagger , and

$$\hat{b}_j^\dagger \rightarrow \sum_{k=1}^n W_{j,k}^\dagger \hat{a}_k^\dagger = \sum_{k=1}^n W_{k,j}^* \hat{a}_k^\dagger. \quad (13)$$

That is to say, even though W does formally not necessarily possess an inverse, the scattering process with exchanged input- and output modes is always described by W^\dagger .

The single-particle evolution governed by the matrix W applies for every single particle. The many-particle state $|\Psi^{2q}(c)\rangle$ thus evolves according to the time-evolution operator $\hat{M}(W)$, which maps a Fock state of particles that were prepared in the input modes, *i.e.* a state given in terms of input-mode creation operators \hat{a}_k^\dagger , to a state in terms of output creation operators \hat{b}_j^\dagger . It thus describes the effect of the single-particle evolution W on the many-particle state. Inserting (11) into (5), we find the effect of $\hat{M}(W)$,

$$\hat{M}(W) |\Psi^{2q}(c)\rangle = \sum_{j_1=1}^d \cdots \sum_{j_N=1}^d c_{j_1, \dots, j_N} \prod_{k=1}^N \left(\sum_{l=1}^n W_{d \cdot (k-1) + j_k, l} \hat{b}_l^\dagger \right) |\text{vac}\rangle. \quad (14)$$

For each summand of the outer multi-sum (which runs over j_1, \dots, j_N), we find

$$\prod_{k=1}^N \left(\sum_{l=1}^n W_{d \cdot (k-1) + j_k, l} \hat{b}_l^\dagger \right) = \sum_{\vec{r}} \left\{ \left[\sum_{\sigma \in S_{\vec{d}(\vec{r})}} \text{sgn}_{\text{B/F}}(\sigma) \prod_{m=1}^N W_{d(k-1) + j_m, \sigma(m)} \left(\hat{b}_{\sigma(m)}^\dagger \right)^{r_m} \right] \right\} \quad (15)$$

where the sum over \vec{r} runs over all possibilities, given W , to distribute the particles among the final modes, $\vec{d}(\vec{r})$ is the mode assignment list, and σ runs over all permutations of this list. The fermionic/bosonic nature of the particles is taken into account by $\text{sgn}_{\text{B/F}}(\sigma)$, which is unity for bosons (B) or the signature of the permutation σ for fermions (F). The time-evolved state $\hat{M}(W) |\Psi^{2q}(c)\rangle$ is thus a coherent superposition of all the possibilities to distribute the particles among the output modes. Similarly to single-particle paths that contribute to an event that exhibits interference, *many-particle* paths are superposed coherently [48]. We illustrate the process with a scattering setup for $N = 4$ particles that each can populate $d = 3$ internal states, in Fig. 1.

1. Properties of the final state

After scattering through the setup, the final, second-quantized state (14) consists of a coherent superposition of all particle arrangements \vec{r} , with corresponding amplitude given by (15). In general, not all components can be interpreted as N -qudit-states, since double occupation of some mode or some group of d modes may occur. We thus need to project the state onto the subspace of post-selected states via the application of $\hat{P}_{1,b}$, and subsequently apply the inverse mapping $\hat{\Omega}_b^{-1}$, where

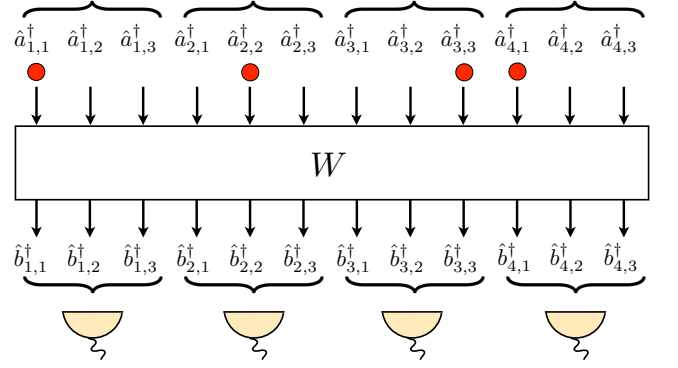


FIG. 1: (color online) **Scattering setup for $N = 4$ qutrit-like ($d = 3$) particles.** The input state corresponds to $\vec{r} = (1, 0, 0, 0, 1, 0, 0, 0, 1, 1, 0, 0)$, $\vec{d}(\vec{r}) = (1, 5, 9, 10)$, and $|\Phi^{1q}(c)\rangle = |1, 2, 3, 1\rangle$.

$\hat{\Omega}_b$ is defined in full analogy to $\hat{\Omega}_a$ in (8), but with interchanged input- and output-creation operators \hat{a}_k^\dagger and \hat{b}_k^\dagger . We eventually obtain the final N -qudit-state

$$|\Phi^{1q}(\tilde{g})\rangle = \hat{\Omega}_b^{-1} \hat{P}_{1,b} \hat{M}(W) \hat{\Omega}_a |\Phi^{1q}(c)\rangle, \quad (16)$$

with a norm that equals the success probability of the procedure (in the following, unnormalized tensors will be denoted as such by a tilde). The normalized state $|\Phi^{1q}(g)\rangle$ describes a d -dimensional, N -partite state, and it is fully defined by its coefficient tensor $g_{j_1 \dots j_N}$ in the representation analogous to (1), which allows us to characterize its entanglement properties with the tools of quantum information theory [17, 58].

D. Entanglement creation and detection

The above-defined mapping between first- and second-quantized representation and the general procedure for the manipulation of entanglement via many-particle scattering are illustrated in Fig. 2. As we show now, the process can be used as a protocol for entanglement generation, detection and projection:

Entanglement generation. Given an initial separable state $|\Phi^{1q}(c)\rangle$, a target entangled state

$$|\Phi^{1q}(\tilde{g})\rangle = \hat{\Omega}_b^{-1} \hat{P}_{1,b} \hat{M}(W) \hat{\Omega}_a |\Phi^{1q}(c)\rangle \quad (17)$$

is generated by scattering and post-selection. The success probability of the entanglement generation process is given by $\langle \Phi^{1q}(\tilde{g}) | \Phi^{1q}(\tilde{g}) \rangle = \left| \hat{P}_{1,b} \hat{M}(W) \hat{\Omega}_a |\Phi^{1q}(c)\rangle \right|^2$. For example, Refs. [7, 37, 38] rely on this procedure.

Entanglement detection. Given an entangled initial state $|\Phi^{1q}(c)\rangle$, the scattering process yields a superposition that contains one or several separable (known) *signal states* $|\Phi^{1q}(s^{(k)})\rangle$,

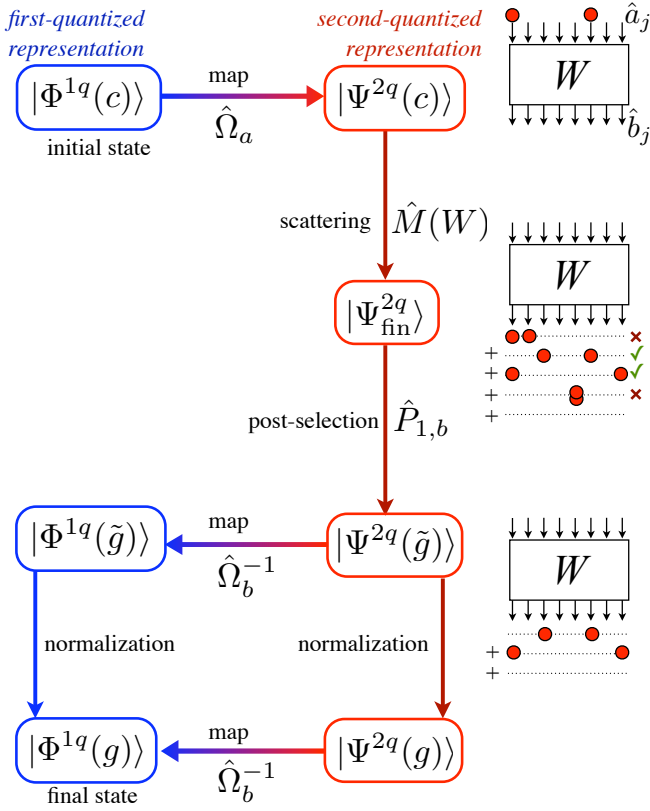


FIG. 2: (color online) **Entanglement manipulation via many-particle scattering.** Given the N -qudit-state $|\Phi^{1q}(c)\rangle$, Eq. (1), the physical second-quantized state is given by Eq. (9), $|\Psi^{2q}(c)\rangle = \hat{\Omega}_a |\Phi^{1q}(c)\rangle$, with the map operator $\hat{\Omega}_a$ given by Eq. (8). The scattering of the particles through the setup is described by $\hat{M}(W)$, Eq. (14), the projection on the subspace of post-selected states is mediated by $\hat{P}_{1,b}$, Eq. (10). The mapping to a first-quantized state occurs via $\hat{\Omega}_b^{-1}$, Eq. (8). The sketch on the right-hand side shows the physical situation for $d = 4$ and $N = 2$. The initial state (upper sketch) contains only one component, it is injected into the scattering setup. The final state contains many coherently superposed components, some of which are not interpretable as N -qudit-states (marked with red crosses). The projector $\hat{P}_{1,b}$ describes the post-selection mechanism, *i.e.* it eliminates the unwanted components and leaves only the post-selected components intact (marked by green crotchets).

i.e. $|\Phi^{1q}(\tilde{g})\rangle = \Omega_b^{-1} \hat{P}_{1,b} \hat{M}(W) \Omega_a |\Phi^{1q}(c)\rangle$ with $\langle \Phi^{1q}(s^{(k)}) | \Phi^{1q}(\tilde{g}) \rangle \neq 0$. All states that are orthogonal to the initial state do not lead to any signal state, such that the detection of signal states is a signature for the initial entangled state.

Entanglement projection. If we start with a superposition of a desired target entangled state $|\Phi^{1q}(g)\rangle$ – as for the entanglement detection scheme – with other undesired components, the detection of a separable signal state $|\Phi^{1q}(s^{(k)})\rangle$ projects the initial superposition onto the target state. This procedure is used, for example, in entanglement swap-

ping protocols [23], or to project atoms into entangled states by measuring the photons emitted by the atoms [33].

The three tasks pose very distinct experimental requirements in general, and they are therefore typically not realized in the same experimental setup. Still, they are fully equivalent in theory: For any number of particles N and any dimensionality of the entanglement carrier d , every created state can also be detected, and every state that can be detected can also be created, in principle.

More formally, a target entangled state $|\Phi^{1q}(g)\rangle$ that is created via the scattering of an initial, separable state $|\Phi^{1q}(c)\rangle$ on a setup W can be detected with the very same separable state as the signal state, via the scattering of the target entangled state on W^\dagger , *i.e.* using the output modes of W as input.

In order to show this, we need to ensure that $|\Psi^{2q}(c)\rangle$ qualifies as a signal state. We thus require (i) a finite detection probability,

$$\langle \Psi^{2q}(c) | \hat{M}(W^\dagger) | \Psi^{2q}(g) \rangle \neq 0. \quad (18)$$

Furthermore, (ii) for all states characterized by g^\perp that are orthogonal to the target state g , the signal state is never produced, *i.e.*

$$\begin{aligned} \forall g^\perp, \text{ with } \langle \Phi^{1q}(g^\perp) | \Phi^{1q}(g) \rangle = 0 : \\ \langle \Psi^{2q}(c) | \hat{M}(W^\dagger) | \Psi^{2q}(g^\perp) \rangle = 0. \end{aligned} \quad (19)$$

Eqs. (18) and (19) are actually satisfied as a direct consequence of $\hat{M}(W^\dagger) = \hat{M}^\dagger(W)$, *i.e.* by the fact that the inverse scattering process is described by W^\dagger (see (12) and (13)).

In full analogy, any state that can be detected can also be created. In order to facilitate our notation in the following, we will always refer to the *entanglement generation* of a desired *target entangled state* – our results can then be applied analogously for entanglement detection and projection.

E. Treatment of internal degrees of freedom

The principle mode of operation being established, it remains to specify the properties of the scattering matrix W for specific physical systems.

The formalism can accommodate setups in which particles are simply redistributed among output modes, without any manipulation of their internal degrees of freedom. We will refer to such setups as *non-polarizing setups* (which does not necessarily imply the restriction to polarization as the internal degree of freedom). Setups that are sensitive to the internal degree of freedom, *i.e.* *polarizing setups*, are also thinkable (such as polarizing beam-splitters, which redirect photons conditioned on their polarization, but which do not change the polarization of the incoming particles). We call a setup that also manipulates the polarization, *e.g.* by using wave

plates, *polarization-manipulating setup*. For these three different types of setups, the scattering matrix W will assume a distinct structure, and distinct target states are accessible.

1. Non-polarizing setups

When photons propagate in free space or scatter off a non-polarizing multiport beam-splitter that treats all internal degrees of freedom equally, we have a propagation of the form

$$\hat{a}_{j,l}^\dagger \rightarrow \sum_{k=1}^N V_{j,k} \hat{b}_{k,l}^\dagger, \quad (20)$$

for particles that are prepared in a spatial mode j and in the internal degree of freedom l , where we distinguished internal and external degrees of freedom for the moment (See Eq. (4)). Each degree of freedom is treated independently and equally, which formally translates into a scattering matrix W that contains one elementary scattering matrix V of dimension $N \times N$,

$$W = V \otimes \mathbb{1}_d. \quad (21)$$

For example, the matrix that describes a non-polarizing beam-splitter,

$$W = \frac{1}{\sqrt{2}} \begin{pmatrix} 1 & 0 & 1 & 0 \\ 0 & 1 & 0 & 1 \\ 1 & 0 & -1 & 0 \\ 0 & 1 & 0 & -1 \end{pmatrix} = \frac{1}{\sqrt{2}} \begin{pmatrix} 1 & 1 \\ 1 & -1 \end{pmatrix} \otimes \mathbb{1}_{(2)} \quad (22)$$

possesses precisely the structure (21). Any scheme that does not manipulate the internal degree of freedom of the scattered particles, such as the ones discussed in [33–35, 37, 38], can be accommodated by a matrix of the form (21).

The entanglement content of the final N -qudit-state depends on the prepared initial internal states of the particles: The multiset of internal states of the particles is not altered, *i.e.* an initial state $|\Phi^{1q}\rangle = |\epsilon_1, \epsilon_2, \dots, \epsilon_N\rangle$ will lead to a final state that can be expressed by superpositions of terms which consist of permutations of the $|\epsilon_k\rangle$ on the output modes. If all $|\epsilon_k\rangle$ are equal, no entanglement can be created.

2. Polarizing setups

The situation is similar for *polarizing setups*, where we allow different dynamics for each internal state, but no coupling between them, *e.g.*, a horizontally polarized photon may be directed to another output mode than a vertically polarized photon, but the polarization of incoming photons is never changed. This model is realistic for degrees of freedom that can be discriminated,

but which cannot be manipulated at will, *i.e.* the device equivalent of a wave plate is not available. The scattering matrix is still a direct sum of scattering matrices, which, however, do not need to be equal,

$$\begin{aligned} W &= V^{(1)} \otimes \text{diag}[(1, 0, \dots, 0)] \\ &+ V^{(2)} \otimes \text{diag}[(0, 1, 0, \dots, 0)] \\ &+ \dots \\ &+ V^{(d)} \otimes \text{diag}[(0, \dots, 0, 1)], \end{aligned} \quad (23)$$

where the $V^{(k)}$ are $N \times N$ matrices and $\text{diag}[\vec{v}]$ is the matrix that contains \vec{v} on the diagonal, whereas all other elements vanish.

For example, a polarizing beam-splitter does not modify polarization, but its action on the modes depends on the polarization state. The matrix

$$\begin{aligned} W_{\text{PBS}} &= \frac{1}{\sqrt{2}} \begin{pmatrix} 1 & 0 & 1 & 0 \\ 0 & 0 & 0 & \sqrt{2} \\ 1 & 0 & -1 & 0 \\ 0 & \sqrt{2} & 0 & 0 \end{pmatrix} \\ &= \frac{1}{\sqrt{2}} \begin{pmatrix} 1 & 1 \\ 1 & -1 \end{pmatrix} \otimes \text{diag}[(1, 0)] \\ &+ \begin{pmatrix} 0 & 1 \\ 1 & 0 \end{pmatrix} \otimes \text{diag}[(0, 1)], \end{aligned} \quad (24)$$

describes a polarizing beam-splitter which reflects and transmits vertically polarized photons with the same probability and always transmits horizontally polarized photons.

3. Polarization-manipulating setups

Finally, a setup which does not only treat different internal degrees of freedom in a distinct way, but also allows their manipulation is described by an unrestricted scattering matrix W . This is experimentally more demanding in general, but routinely done for photon polarization, with the help of phase shifters, polarization rotators (*e.g.* implemented by the combination of quarter- and half-wave-plates) and polarizing beam-splitters.

F. Effective degrees of freedom and independence of initial state

1. Multiple mode occupation

At first sight, the formalism seems to restrict severely the types of setups with which entanglement is produced: Often, the *initial* state in an experiment does not possess an interpretation as N -qudit-state in the quantum information abstraction, such that no $|\Phi^{1q}\rangle$ can be given. For example, a many-particle state with all particles in the

same spatial mode is scattered on several beam-splitters in [14], which permits the creation of a permutation-symmetric entangled state.

Such initial multiple population is, however, unproblematic: If two particles are prepared in the same mode, we can equally well describe them by a setup in which they formally occupy two *distinct* modes, but for which the two rows of the matrix representation that describes the evolution of the particles are identical. We can thus absorb such initial preparation of particles into the matrix W .

2. Local unitary operations

All local operations that act independently on each particle in the input or in the output modes, *i.e.* local unitary operations [63, 64], can also be absorbed by the scattering matrix:

$$W = \left(L_1^{(i)} \oplus \cdots \oplus L_N^{(i)} \right) W_0 \left(L_1^{(f)} \oplus \cdots \oplus L_N^{(f)} \right), \quad (25)$$

where $L_k^{(i)}$ and $L_l^{(f)}$ are $d \times d$ -matrices that describe local unitary transformations on the k th spatial input- and on the l th spatial output mode, respectively. We can therefore restrict our analysis to a unique initial state $|\Phi^{1q}\rangle = |1, 1, 1, \dots, 1\rangle$, in which all particles are prepared in the same internal state and in distinct spatial modes. All relevant parameters can be varied by the entries of the scattering matrix W .

III. STATE REPRESENTATION AND COMBINATORIAL BOUNDS

Having established the physical process for entanglement generation as well as the possible structures of the scattering matrix W , we now proceed to the explicit representation of the states that can be generated, given an initially separable state. The form for polarization-manipulating setups will be the most general one, while we find a simpler representation for non-polarizing setups. In all cases, elementary algebraic manipulations allow us to obtain a form from which the maximal Schmidt rank, *i.e.* the maximal number of separable components of a state, can be read off.

A. Non-polarizing setups and permutation representation

For a non-polarizing setup, we are given a scattering matrix of the form (21), with an $N \times N$ -matrix V as non-trivial ingredient. Any separable initial state can be written as

$$|\Phi^{1q}(c)\rangle = |\epsilon_1, \dots, \epsilon_N\rangle, \quad (26)$$

where $|\epsilon_k\rangle$ denotes the internal state of the k th particle.

Since, by assumption, the internal degrees of freedom cannot be modified by the setup, the multiset of internal states that the particles are initially prepared in, $\{|\epsilon_1\rangle, \dots, |\epsilon_N\rangle\}$, remains invariant under scattering. Consequently, the first-quantized final state will always possess a *permutation representation*,

$$|\Phi^{1q}(\tilde{g})\rangle = \sum_{\sigma \in S_N} \bar{g}_\sigma \left(\bigotimes_{j=1}^N |\epsilon_{\sigma(j)}\rangle_j \right), \quad (27)$$

where \bar{g}_σ is a coefficient that depends on the permutation σ , and all possible distributions of the single-particle states $|\epsilon_j\rangle$ on the spatial output modes are taken into account. By a parameter-counting argument, we see that not every state can be represented by the form (27): The number of parameters (the number of \bar{g}_σ) is $N!$, whereas N^N parameters are required for the description of a general state of N particles each associated with an N -dimensional degree of freedom. For constant coefficients $\bar{g}_\sigma = \bar{g}$, the state (27) is fully permutation-symmetric. In particular, any permutation-symmetric state with $d = 2$ can be written in the *Majorana-representation* [65, 66], *i.e.* one can then always find a multiset $\{|\epsilon_j\rangle\}$ to represent it in the form (27). Physically speaking, every permutation-symmetric state of qubits can be created with beam-splitters and phase-shifters [36].

In the present scattering scenario, the coefficients \bar{g}_σ cannot be adjusted independently, but they are given as a function of the scattering matrix elements $V_{k,l}$, and they depend on the type of particles (bosons or fermions). Each component $|\epsilon_{\sigma(1)}, \dots, \epsilon_{\sigma(N)}\rangle$ in the state (27) obtains the amplitude of the corresponding *many-particle path*, for which the $\sigma(j)$ th particle falls into the j th spatial output mode. Consequently, applying $\hat{P}_{1,b}$ to the state in (15) and identifying the coefficients \bar{g}_σ in the equivalent representation (27) yields

$$\bar{g}_\sigma = \text{sgn}_{B/F}(\sigma) \prod_{j=1}^N V_{\sigma(j),j}, \quad (28)$$

where $\text{sgn}_{B/F}(\sigma)$ denotes the signature of the permutation σ for fermions, and is always unity in the case of bosons. That is to say, the final state for non-polarizing setups is a superposition of all possibilities to distribute the particles prepared at the N spatial input modes over the N spatial output modes. The amplitude for each of these permutations is given by the product of the scattering matrix elements as defined in (28).

B. Polarizing and polarization-manipulating setups

For polarizing setups, which do not manipulate the internal degrees of freedom of the particles, one cannot use the permutation representation to express the final state, since particles in distinct internal states can behave

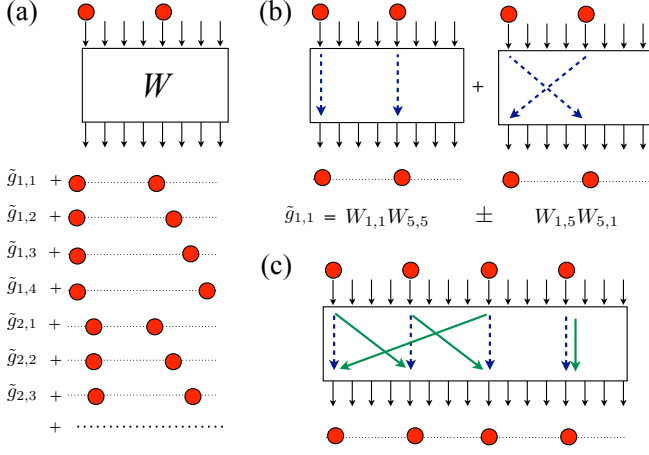


FIG. 3: (color online) **Superposition of many-particle paths.** (a) A state of $N = 2$ particles that carry a $d = 4$ -dimensional degree of freedom is characterized by the coefficient tensor \tilde{g} , which indicates the amplitude of each basis state. (b) Each basis state (here: $|1, 1\rangle$) is fed by the many-particle paths that contribute to the respective event. (c) In general, there are up to $N!$ of these paths, we show here two exemplary paths for $N = 4$ particles.

differently and the single-particle states $\{|\epsilon_k\rangle\}$ are not preserved. We therefore treat this case together with polarization-manipulating setups. In general, the target state's first-quantized notation is

$$|\Phi^{1q}(\tilde{g})\rangle = \sum_{j_1=1}^d \cdots \sum_{j_N=1}^d \tilde{g}_{j_1, \dots, j_N} |j_1, j_2, \dots, j_N\rangle. \quad (29)$$

For an initial state with all particles in the internal state $|j_k = 1\rangle$ (remember that arbitrary local operations on the initial qudits can be absorbed in the scattering matrix W , as described in Section II F, we evaluate the coefficients $\tilde{g}_{j_1, \dots, j_N}$ via the application of $\hat{P}_{1,b}$ onto (15):

$$\tilde{g}_{j_1, \dots, j_N} = \sum_{\sigma \in S_N} \text{sgn}_{B/F}(\sigma) \prod_{k=1}^N W_{d \cdot (\sigma[k]-1)+1, d(k-1)+j_k}. \quad (30)$$

The bound can be derived from the representation of the final state $|\Phi^{1q}(\tilde{g})\rangle$, which reads, according to (29,30),

$$|\Phi^{1q}(\tilde{g})\rangle = \sum_{j_1=1}^d \cdots \sum_{j_N=1}^d \sum_{\sigma \in S_N} \text{sgn}_{B/F}(\sigma) \prod_{k=1}^N W_{d(\sigma[k]-1)+1, d(k-1)+j_k} |j_1, \dots, j_N\rangle, \quad (32)$$

and which can be re-written as

$$|\Phi^{1q}(\tilde{g})\rangle = \sum_{\sigma \in S_N} \text{sgn}_{B/F}(\sigma) \left[\otimes_{m=1}^N \left(\sum_{j_m=1}^d W_{d(\sigma[m]-1)+1, d(m-1)+j_m} |j_m\rangle_m \right) \right], \quad (33)$$

where $|j_m\rangle_m$ denotes the state of the m th qudit prepared in the j_m th internal state. In other words, every state that is created by many-particle interference can be written as the sum of $N!$ (from the sum over all permutations σ) separable terms of the form (3).

For the interpretation of (30), we can apply an intuitive picture of many-particle paths [48], which is also illustrated in Fig. 3: Many distinct many-particle paths contribute to post-selected events with one particle per group of modes, and the entanglement in the final state originates from this superposition of distinct paths [57] (see Fig. 3 (a)). Each separable basis state $|j_1, j_2, \dots, j_N\rangle$ in the final state representation is fed by up to $N!$ distinct contributions (see (b) and (c)): The particle initially in mode $d \cdot (\sigma[k] - 1) + 1$ is redirected to mode $d \cdot (k-1) + j_k$, and the product of the corresponding amplitudes gives the many-particle amplitude that contributes to this specific scattering process. All these amplitudes are superimposed and interfere (see (b)), and their sum equals the coefficient $\tilde{g}_{j_1, \dots, j_N}$.

C. Combinatorial bounds

With the explicit state representations at hand (see (27) and (30)), we can now map the task “given a certain infrastructure, can we create the state $|\Phi^{1q}(h)\rangle$ starting from a separable state?” to a concrete mathematical problem: It corresponds to the set of d^N equations

$$\tilde{g}_{j_1, \dots, j_N} = \eta h_{j_1, \dots, j_N}, \quad (31)$$

for the matrix elements $W_{k,l}$, where the $\tilde{g}_{j_1, \dots, j_N}$ are given by (30) and η accounts for the sub-normalization of the \tilde{g} . In general, this task is manifestly rather difficult, since the coefficients $\tilde{g}_{j_1, \dots, j_N}$ are highly non-linear functions of the unknown parameters $W_{k,l}$.

Still, the explicit representation (30) permits the identification of limitations that apply to entanglement generation via many-particle interference, in terms of an upper bound for the generalized Schmidt rank [49].

This result immediately yields an upper bound for the Schmidt rank $R(|\Phi^{1q}(\tilde{g})\rangle)$ of the state $|\Phi^{1q}(\tilde{g})\rangle$,

$$R(|\Phi^{1q}(\tilde{g})\rangle) \leq N!, \quad (34)$$

where the Schmidt rank is the minimal necessary number of summands in the representation of $|\Phi^{1q}\rangle$ as a sum of separable states [49]. This fundamental bound for multipartite entangled states that are generated via many-particle interference can be understood via an intuitive combinatorial argument: Each possibility to distribute the particles among the output modes can only contribute one term in the representation of the emerging state. Thereby, we have established a link between the number of many-particle paths and an entanglement measure, namely the generalized Schmidt number, which is defined as $\log_2 R(|\Phi^{1q}(\tilde{g})\rangle)$ [49].

D. Initial states with multiple occupation

Through our reference to (30), we assumed in Section III C above that the initial state is the N -qudit-state $|\Phi^{1q}\rangle = |1, \dots, 1\rangle$, *i.e.* a state with exactly one particle in each group of d modes. If an initial physical state with larger occupancy is used (which does not admit an interpretation as N -qudit-state and which is only admissible for bosons), a tighter bound emerges. In this case, we can formally use the same initial state $|\Phi^{1q}\rangle$, but we account for the multiple occupation by equating the corresponding rows of the scattering matrix (see Section II F). When r_j is the occupation number of each mode ($\sum_{j=1}^n r_j = N$), the scattering matrix W effectively reflects this multiple occupation by possessing r_j equal rows. The outer sum in (33) reduces to only $N!/(\prod_{j=1}^n r_j!)$ terms, since for each $\sigma \in S_N$, there are $\prod_{j=1}^n r_j!$ permutations that leave the summand

$$\otimes_{m=1}^N \sum_{j_m=1}^d W_{d(\sigma[m]-1)+1, d(m-1)+j_m} |j_m\rangle_m \quad (35)$$

invariant. This can, again, be interpreted in a picture of many-particle paths: When several particles are initially prepared in the very same state, a permutation of these particles does not lead to a distinct many-particle amplitude. Therefore, the number of distinct many-particle amplitudes is reduced by a factor $\prod_{j=1}^n r_j!$.

As an extreme example, it is not possible to extract entanglement from an ideal Bose-Einstein-Condensate (BEC), which is described by

$$|\Psi_{\text{BEC}}^{2q}\rangle = \frac{(\hat{a}_1^\dagger)^N}{\sqrt{N!}} |\text{vac}\rangle, \quad (36)$$

i.e. a state of N particles with all particles in the same mode, since $N!/(\prod_{j=1}^n r_j!) = 1$ for $\vec{r} = (N, 0, \dots, 0)$. Post-selected events with one particle in each output

mode can only be reached via one many-particle path, such that the Schmidt rank of the resulting state is always unity. This generalizes the result of [67], where it was found that no entanglement can be extracted from a BEC when no manipulations of the internal state dynamics are allowed. One consequence of our results is that even such manipulation on the internal degrees of freedom is of no help.

E. Entangled initial states

In turn, the use of an entangled initial state allows one to increase the upper bound on the Schmidt rank of the final state: The combinatorial bound applies to every single separable term in the representation of the initial state in its generalized Schmidt form. Given an initial Schmidt rank R_{in} , the combinatorial bound is extended up to $R_{\text{in}}N!$. In other words, the concatenation of many-particle interference processes and post-selection can be used to increase the Schmidt rank step by step-wise, by a factor of up to $N!$ in each step.

F. Interpretation

The combinatorial bound should not be regarded as a purely quantum phenomenon: It also applies to a classical probabilistic process in which N distinguishable objects are randomly distributed to N observers. The number of distinct outcomes that the N observers can experience is, again, bound by $N!$, just like the generalized Schmidt rank is according to (34). If some of the objects are identical, permutations that exchange these objects do not lead to inequivalent events, just like the multiple initial occupation of any mode reduces the rank, as discussed in Section III D. The quantum properties of bosons and fermions, *i.e.* their (anti)-commutation relations which provide an alternating sign for fermions in the sums (15,30), do not play any role, and the bound applies equally well to both species. It is, furthermore, independent of the presence of polarizing components. In contrast, we will see that bosons and fermions indeed do hold a different potential for entanglement generation, as will be shown by means of the dimensionality of the manifold of accessible states in the next Section.

IV. DIMENSION OF THE MANIFOLD OF ACCESSIBLE STATES

For systems of large dimensions $d \gtrsim N$, the combinatorial bound (34) dominates the set of accessible states. By a parameter-counting argument, however, we see that not all states can be created when the number of particles N is large, for *any* dimension $d \geq 2$: On the one hand, the number of complex parameters for a general N -partite quantum state with a d -dimensional internal

degree of freedom is d^N (including normalization and global phase). On the other hand, the number of complex parameters of the scattering matrix W that controls the final state (32) is only $d \cdot N^2$: We are given the initial state $|\Phi^{1q}\rangle = |1, 1, \dots, 1\rangle$, and only the matrix elements $W_{(k-1)d+1,j}$ with $1 \leq k \leq N$ and $1 \leq j \leq dN$ appear in the sum (32). The exponential growth of the parameters of entangled states with the number of involved particles reflects the complexity of many-particle quantum mechanics, which cannot be reproduced by the limited amount of free parameters in the interference-based setup under investigation.

A. Fermionic and bosonic bounds

The rough upper bound provided by the above parameter-counting argument can be ameliorated by studying the structure of the state coefficients in (32) in more detail. This allows us to obtain a tight upper bound for the dimensionality of the manifold of accessible states. We denote by $\Xi_{F(B)}$ the manifold of states of the form (32) for fermions (bosons), which is spanned by all matrices W . In contrast to the combinatorial bound, we find a striking difference between bosons and fermions. The derivation of the bounds is presented in Appendix B. For fermions, we find

$$\dim(\Xi_F) \leq (d-1)N^2 - N + 2, \quad (37)$$

while for bosons, we have

$$\dim(\Xi_B) \leq dN^2 - 2N + 2. \quad (38)$$

Roughly speaking, the computation of scattering amplitudes for fermions involves the evaluation of determinants, which is facilitated by the symmetry properties of this function, in particular, by the property $\det(AB) = \det(A)\det(B)$. Scattering amplitudes for bosons instead involve the *permanent* [68–70], a complex-valued function of matrices similar to the determinant, but that does not feature equivalent symmetry properties. The number of effective parameters for bosons is therefore larger than for fermions.

The bosonic bound (38) is only applicable when it is smaller or equal to the dimension d^N of the total state space. For $N = 2$, and for $d = 2, N = 3, 4$, the bound exceeds the total dimensionality of the many-particle Hilbert-space, N^d ; it is thus not relevant. For large systems, the bound strongly limits the manifold of accessible states, as we will also see in the next Section in Table II.

B. Tightness of bounds

The established inequalities (37) and (38) provide upper bounds to the dimensionality of the manifold of entangled states that can be created by fermions and bosons, respectively. For small dimensions d and small

particle numbers N , we found numerically that the equality holds in (37) and (38). One thus indeed possesses a number of independent parameters that corresponds to the right-hand side of (37), (38). For this purpose, we evaluated the rank of the Jacobian

$$\frac{\partial g_{j_1, \dots, j_N}}{\partial W'_{l,k}}, \quad (39)$$

for random scattering matrices W . The results are shown in Table II: they always match the encountered upper bound.

	N Bosons								N Fermions							
	2	3	4	5	6	7	8		2	3	4	5	6	7		
$d = 2$	<u>4</u>	<u>8</u>	<u>16</u>	<u>32</u>	62	86	114		<u>4</u>	<u>8</u>	14	22	32	44		
3	(8)	23	42	67	98				8	17	30	47	68			
4	(12)	32	58	92	134				12	26	46	72				
5	(16)	41	74	117					16	35	62	97				

TABLE II: (color online) **Numerically obtained lower bounds for the dimensionality $\dim(\Xi_{B/F})$ of the accessible set of states, for unconstrained setups, according to Eq. (39).** Blue underlined numbers indicate combinations of d and N which are not subject to any constraint, *i.e.* all entangled states can be created via many-particle interference. Red numbers (in parenthesis) refer to combinations of (d, N) for which the combinatorial bound (34) is tighter than the bosonic bound (38). All numerically inferred lower bounds match the analytically obtained upper bounds (37) and (38) or the maximal dimensionality that can be attained according to the combinatorial bound (34).

C. Interpretation and consequences

Our results on the effective number of parameters for bosons and fermions demonstrate that the combinatorial bound (34) is not the only restriction to the set of accessible states. The complexity of general multi-partite entangled states cannot be reproduced in interference-based setups, simply due to the limited number of parameters. When fermions are used, the symmetry properties of the determinant reduce the effective number of parameters in comparison to bosons. Indeed, the computation of fermionic many-particle scattering amplitudes is computationally much less demanding than the corresponding task for bosons [70], and this computational complexity is reflected in the larger manifold for bosons.

This larger manifold of states that are accessible for bosons comes at an expense: For fermions, the entanglement generation process is assisted by the Pauli principle, which forbids multiply occupied modes that correspond to unsuccessful events. The average tendency of bosons to bunch, on the other hand, enhances unsuccessful events. For larger dimensions d , the total number of modes n increases, and the Pauli principle becomes less dominating, as well as the bunching tendency of bosons is

less prominent: Due to the lower particle density, multiply occupied states become less probable in general, since many more possible states with at most one particle in each of the n modes emerge. Simultaneously, the quotient of the bounds to the manifold dimension of fermions to the manifold dimension of bosons, $\dim(\Xi_F)/\dim(\Xi_B)$ (see (37) and (38)), converges to unity for $d \rightarrow \infty$, *i.e.* the advantage of bosons with respect to fermions regarding the dimensionality is jeopardized. In other words, there is a trade-off between success probability and the dimensionality of the accessible manifold.

Given the dimensionality estimate (38) for qubits that are carried by bosons, we can expect that all four-partite and five-partite qubit states can be created with linear optics, with experiments similar to [13, 14, 18, 31, 71]. For six photons, we find that only 62 of a total of 64 dimensions are spanned. Given the manifold possibilities to create entangled six-photon states by parametric down-conversion processes, it is, however, possible that one may find ways to create the inaccessible states starting from entangled initial states.

Significant progress has been achieved in the design of alternative, efficient single-photon sources [72–74]. However, our results indicate that extending experiments to larger particle numbers is not only limited by technological issues, but fundamental limitations to the accessible states will severely come into play for large particle-numbers. For example, for $N = 8, d = 2$, Ξ_B has only 114 dimensions, significantly less than the dimension of the Hilbert space, 256. In analogous experiments with fermions, *e.g.* with cold atoms in optical lattices, one will experience a bound for the accessible states already for four particles.

For bosons, the inclusion of loss in the setup, *i.e.* the use of non-unitary scattering matrices W , permits the generation of states that are inaccessible for unitary matrices: Consider a lossless setup described by the unitary $dN \times dN$ matrix W , *i.e.* the matrices X, Y, Z in the representation (12) are empty. The number of parameters that affect the relevant $dN \times N$ -dimensional sub-matrix W' of W can be inferred by counting the Euler-angles of W that do not affect W' . The total number of complex Euler-angles that define W amounts to $Nd(Nd-1)$, while $N(d-1)(N(d-1)-1)$ of these are irrelevant for W' . The difference yields the number of parameters K ,

$$K = \left(d - \frac{1}{2}\right) N^2 - \frac{N}{2}. \quad (40)$$

This value is exceeded by the dimensionality of bosons, $\dim(\Xi_B)$ (38). The inclusion of lossy setups (or, equivalently, of the multiple population of modes in the initial state, see Section III D) thus offers advantages over lossless, unitary setups. For fermions, however, the number of parameters of a unitary matrix U is larger than our dimensional bound, $\dim(U) > \dim(\Xi_B)$, which suggests that no advantage is accomplished for fermions by including loss in the setup.

V. CONCLUSIONS AND OUTLOOK

The emergence of quantum correlations from the propagation and detection of bosons and fermions can be described by the presented unified formalism, which also provides an intuitive interpretation: Particles are redistributed from input modes to output modes, and the probability to fall into each output mode depends on the initial state of the particle. This process has a purely classical analogy: The random distribution of distinguishable objects to parties/observers also leads to classical correlations between the objects that are subsequently observed by the parties. Here, we have considered the coherent version of this process, and the resulting correlations are of quantum nature.

The physical process of *redistributing* particles among observing parties is the very basis for a panoply of experiments and theoretical schemes. We aimed at providing a common framework for the creation and detection of entangled states via the deletion of which-way information, and obtained an explicit representation (30) of all states that can be created or detected via linear optics setups. Depending on the experimental capabilities, *i.e.* whether the device that is equivalent to a polarizing beam-splitter can be implemented or not, the form of the scattering matrix is very different, and different types of states can become accessible. The combinatorial bound, however, cannot be circumvented. The computational complexity of the permanent and determinant, which appear in the scattering amplitudes for bosons and fermions, respectively, is reflected by the effective number of parameters that are available to generate entangled states.

In general, any experiment in which particle-carried entanglement is created without direct interaction between the constituents can be described by a scattering matrix W , and the resulting state has a representation of the form (30). Given the experimental limitations, one can thus optimize the creation of entanglement by finding the optimal matrix W .

Some proposals that encode qudits in a different way than we have assumed here can circumvent the combinatorial bound, and can reach states that are not represented by (30). For example, mode-entanglement [75–77], *i.e.* entanglement in the particle-number degree of freedom, is not subject to the bound, as well as schemes in which qudits are carried by several particles instead of a single one [50, 78–80].

The prospect for many-particle entanglement creation with photons is restricted by the dramatic decrease of the success rate for increasing particle number N , since unsuccessful events with multiply occupied spatial output modes then become more and more probable, although there are approaches to tackle this inefficiency by using the time-bin as an additional discriminating degree of freedom [81]. The very understanding of multipartite entanglement being a widely open issue, the state representation (30) offers a way to understand at least the structure of the states that can be created via the

exploitation of the indistinguishability of the particles. In particular, completely anti-symmetric and completely symmetric states are contained in the general states for fermions and bosons, respectively. Since these special classes are rather well understood, the hope is fed that one may characterize the more general state (30) via entanglement measures or via its non-local properties, and thereby also characterize the potential of non-linear single-photon schemes [82].

In particular, the question arises whether the manifold of accessible states for fermions is a *submanifold* of the accessible states for bosons. This appears suggestive from the clear hierarchy of the bounds (37,38) for the dimensionalities that we have encountered, but, in turn, also questionable, since fully symmetric and fully anti-symmetric states which are accessible for bosons and fermions, respectively, when the scattering matrix V is the constant matrix (see Eq. (A3)) possess very distinct entanglement properties [83]. Also the influence of restrictions on the setup, *i.e.* the use of non-polarizing setups instead of the unconstrained form, remains to be studied. The answers to these questions may contribute further to an understanding of the structure of multipartite entangled states.

Acknowledgments

We would like to thank Hyang-Tag Lim and Young-Sik Ra for enlightening discussions. M.C.T. acknowledges support by German National Academic Foundation, A.B. acknowledges partial support through the EU-COST Action MP1006 “Fundamental Problems in Quantum Physics” and through DFG Research Unit 760.

Appendix A: Accommodation of existing schemes

Many existing schemes that seem rather unrelated to each other at first sight can be put onto a common footing. In the following, we give an exemplary overview over various methods that can be described by the formalism described in this article, which stresses the shared underlying physical roots of the different theoretical and experimental methods.

1. Theoretical proposals

a. Scattering on the Fourier multiport

Several multipartite entangled states can be created with Fourier multiport devices via the scattering of bosons that are prepared in certain initial states [38]. The setup is non-polarizing, with

$$W = V \otimes \mathbb{1}_2, \text{ and } V = U^{\text{Fou}}, \quad (\text{A1})$$

where $(U^{\text{Fou}})_{j,k} = e^{i\frac{2\pi}{N}(j-1)(k-1)}$ is the Fourier matrix. No devices that are equivalent to polarizers need to be used, such that the infrastructure is independent of the specific degree of freedom that is entangled. The final state reads (as given in (27))

$$|\Phi^{1q}(\tilde{g})\rangle = \sum_{\sigma \in S_N} \left(\prod_{j=1}^N U_{\sigma(j),j}^{\text{Fou}} \right) \otimes_{k=1}^N |\epsilon_{\sigma(k)}\rangle_k, \quad (\text{A2})$$

where the $|\epsilon_k\rangle$ are the initial internal states of the bosons at the input modes. In particular, a W-type state [84] can be created by preparing one photon in horizontal, $|H\rangle$, and the remaining $N - 1$ photons in vertical polarization, $|V\rangle$. Due to the cyclic invariance of the Fourier matrix, it is ensured that all amplitudes of the distinct components with the j th particle in horizontal polarization ($|H, V, V, V, \dots\rangle$, $|V, H, V, V, \dots\rangle$, etc.) enter with the same amplitude. For four particles, a GHZ-state of four photons can equally well be produced with the initial state $|V, V, H, H\rangle$.

b. Free space propagation

A free-space photon-propagation scheme [33–37] allows to generate a variety of entangled states. Both, entanglement projection (with consequent entanglement swapping) [35], and entanglement creation [37] are possible. In all cases, photons propagate in free space, and they are collected by an array of N detectors, each of which projects the incoming photon onto a certain polarization state. Each photon has the same probability to be absorbed by each detector. In particular, Dicke states, *i.e.* states $|S, m\rangle$ which are simultaneous eigenstates of the total squared spin operator \hat{S}^2 and its z -component \hat{S}_z , with eigenvalues S and m , respectively, are accessible [33]. More generally, all permutation-symmetric states can be created [37], and – with few modifications of the scattering matrix – all 2^N distinct total angular momentum eigenstates [34, 85].

The scattering matrix W is non-polarizing, and its submatrix V (see (21)) is the constant matrix with $V_{j,k} = \sqrt{p}$, where p is the probability that a photon is registered by the detector. For the state representation, we can use (27) to find

$$\begin{aligned} |\Phi_{\text{fin}}^{1q}\rangle &= \sum_{\sigma \in S_N} \left(\prod_{j=1}^N V_{\sigma(j),j} \right) \otimes_{k=1}^N |\epsilon_{\sigma(k)}\rangle_k \\ &= \sqrt{p^N} \sum_{\sigma \in S_N} \otimes_{k=1}^N |\epsilon_{\sigma(k)}\rangle_k. \end{aligned} \quad (\text{A3})$$

In other words, a fully permutation-symmetric state emerges [43, 47, 65, 86, 87].

2. Experimental implementations

Many qualitatively distinct classes of entangled states [6, 9, 11, 88] have been realized in experiments that employ photons as carriers of entanglement. In order to exemplify the versatility of many-photon entanglement generation, we discuss in more detail the projection onto a tripartite entangled GHZ-state [89] and the versatile tunability of distinct SLOCC classes for four-photon states [31].

a. GHZ entanglement swapping

Entanglement swapping among three parties was experimentally demonstrated [89] with the setup reproduced in Fig. 4. A laser pulse that induces parametric down-conversion on three aligned crystals (BBO in the Figure) results in the creation of

$$|\Phi_{\text{ini}}^{1q}\rangle = |\Phi^+\rangle_{1,2} \otimes |\Phi^+\rangle_{3,4} \otimes |\Phi^+\rangle_{5,6}, \quad (\text{A4})$$

where $|\Phi^+\rangle_{k,l}$ denotes the $|\Phi^+\rangle$ Bell-state in the polarization degree of freedom, shared between the photons in the spatial modes k and l :

$$|\Phi^+\rangle_{k,l} = \frac{1}{\sqrt{2}} (|H, H\rangle_{k,l} + |V, V\rangle_{k,l}). \quad (\text{A5})$$

Photons 1, 3 and 5 are then projected onto a GHZ-state,

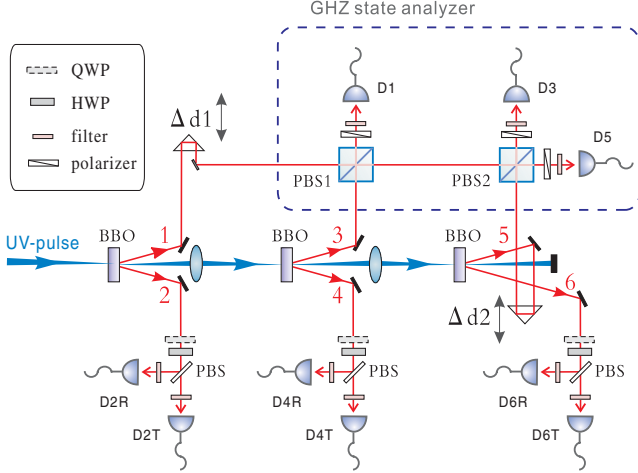


FIG. 4: (color online) **GHZ entanglement projection.** The photon pairs (1,2), (3,4) and (5,6) are initially polarization-entangled, as described by Eq. (A4). By the projection of photons 1, 3 and 5 onto the GHZ-state (at detectors D1, D3, D5, by the implementation of the scattering matrix (A8)), photons 2, 4, and 6 are also left in the GHZ-state. Courtesy of C.-Y. Lu, T. Yang and J.-W. Pan [89].

$$|\text{GHZ}\rangle_{1,3,5} = \frac{1}{\sqrt{2}} (|H, H, H\rangle + |V, V, V\rangle), \quad (\text{A6})$$

via a GHZ-state analyzer [90] (dashed area in Fig. 4). The polarizing beam-splitters (PBS) reflect vertically polarized photons and transmit horizontally polarized ones, while the polarizers after the PBS only transmit the $|+\rangle = (|H\rangle + |V\rangle)/\sqrt{2}$ -component of the light field. The resulting scattering matrix W_{GHZ} that describes the propagation of the photons in the input modes

$$|H\rangle_1, |V\rangle_1, |H\rangle_3, |V\rangle_3, |H\rangle_5, |V\rangle_5, \quad (\text{A7})$$

to the detectors $D1, D3, D5$ reads

$$W_{\text{GHZ}} = \frac{1}{\sqrt{2}} \begin{pmatrix} 0 & 0 & 1 \\ 1 & 0 & 0 \\ 1 & 0 & 0 \\ 0 & 1 & 0 \\ 0 & 1 & 0 \\ 0 & 0 & 1 \end{pmatrix}, \quad (\text{A8})$$

i.e. it corresponds to a combined action of polarizing beam-splitters and polarizers, as described in Section II E 2. The state at modes 2,4 and 6 is then measured in different bases to verify quantum correlations. The path lengths $\Delta d1$ and $\Delta d2$ (see Figure) are adjusted by monitoring four-photon and six-photon coincident events. As discussed in Section II D, the matrix W_{GHZ}^\dagger can also be used for the *creation* of a GHZ-state.

b. Family of four-photon states

The setup for the projection onto the GHZ state discussed above projects onto one very specific state. One can, however, also scan through entire families of entangled states by tuning the parameters of the scattering matrix W . This was realized in a four-photon experiment [31, 71], in which one starts with a four-photon state created via parametric down-conversion, which reads

$$|\Psi_{\text{ini}}^{2q}\rangle = \frac{1}{2\sqrt{3}} \left(\left(\hat{a}_{1,H}^\dagger \hat{a}_{2,V}^\dagger \right)^2 + \left(\hat{a}_{1,V}^\dagger \hat{a}_{2,H}^\dagger \right)^2 + 2\hat{a}_{1,H}^\dagger \hat{a}_{1,V}^\dagger \hat{a}_{2,H}^\dagger \hat{a}_{2,V}^\dagger \right) |\text{vac}\rangle, \quad (\text{A9})$$

i.e. there are always two photons of horizontal and of vertical polarization, respectively, and there is one component with the photons distributed among all four physical modes and two components with two photons in the same mode.

A variable polarization-rotation with angle γ is applied to the spatial mode \hat{a}_1^\dagger (see $\text{HWP}(\gamma)$ in Fig. 5, we identify (a) and (b) in the figure with the first and second spatial input modes). The two spatial modes are then combined at a polarizing beam-splitter (PBS in the figure) that reflects vertically polarized photons. The polarization in one of the outgoing modes ((c) in the figure) is then flipped by a half-wave plate ($\text{HWP}(\pi/4)$), and the spatial modes are split into two parts each, such that

there are four final modes which can carry two possible polarizations (in the figure: (e), (f), (g), (h)). The scattering matrix that describes the evolution of the four distinct input modes (1H, 1V, 2H, 2V) to the output modes (1H, 1V, ..., 4H, 4V) reads

$$W = \frac{1}{\sqrt{2}} \begin{pmatrix} -s & 0 & -s & 0 & c & 0 & c & 0 \\ c & 0 & c & 0 & s & 0 & s & 0 \\ 0 & 1 & 0 & 1 & 0 & 0 & 0 & 0 \\ 0 & 0 & 0 & 0 & 0 & 1 & 0 & 1 \end{pmatrix}, \quad (\text{A10})$$

where $s = \sin(2\gamma)$ and $c = \cos(2\gamma)$, *i.e.* the setup manipulates the polarization, and it depends on the polarization rotation angle γ . The result of a post-selected event with one particle in each output mode is a final state of the form

$$|\tilde{\Phi}^{1q}\rangle = \frac{1}{2\sqrt{3}} \left(\sin^2(2\gamma) |\text{GHZ}_4\rangle + \frac{\cos(4\gamma)}{2} |\Psi^+\rangle_{1,2} \otimes |\Psi^+\rangle_{3,4} \right), \quad (\text{A11})$$

i.e. it is a coherent superposition of a bi-separable double-Bell state and a four-particle GHZ-state, where

$$|\Psi^+\rangle_{k,l} = \frac{1}{\sqrt{2}} (|H, V\rangle_{k,l} + |V, H\rangle_{k,l}), \quad (\text{A12})$$

$$|\text{GHZ}_4\rangle = \frac{1}{\sqrt{2}} (|H, H, V, V\rangle + |V, V, H, H\rangle). \quad (\text{A13})$$

The success probability is $(\cos(4\gamma)^2 + 2\sin(2\gamma)^4)/12$. The parameter γ allows one to tune through several SLOCC-inequivalent entangled states of four photons [91].

Appendix B: Derivation of bounds on the dimensionality

We derive here the upper bounds (37), (38) for the dimensionality $\dim(\Xi_F)$ and $\dim(\Xi_B)$ of the manifold of accessible states, respectively. For this purpose, we regroup the matrix elements of W that appear in the state representation (30) in a smaller matrix W' of dimension $N \times dN$:

$$W'_{k,j} = W_{(k-1)d+1,j}, \quad (\text{B1})$$

such that W' contains all relevant parameters (remember from Section II F 2 that we can always assume the initial separable state $|\Phi^{1q}\rangle = |1, \dots, 1\rangle$). Formally speaking, in (32) the dN^2 elements of the scattering matrix $W'_{j,k}$ are mapped onto the d^N -dimensional space of the $\tilde{g}_{j_1, \dots, j_N}$. The dimensionality of the accessible manifold $\Xi_{F/B}$ is the effective number of complex parameters that are necessary to describe the $\tilde{g}_{j_1, \dots, j_N}$.

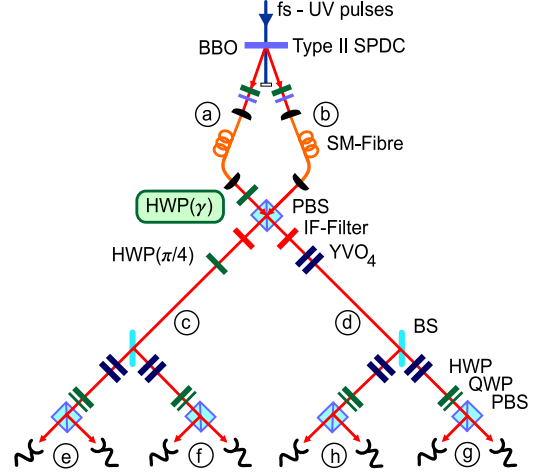


FIG. 5: (color online) **Creation of a family of entangled four-photon states.** Two input modes (a) and (b) are combined at the polarizing beam-splitter (PBS), and they are subsequently split into four modes (e,f,g,h) by two additional beam-splitters (BS). The initial state (A9) is thus scattered on a setup which implements (A10). The final quantum-information state (A12) depends on the polarization-rotation parameter γ . Courtesy of W. Wieczorek, C. Schmid, N. Kiesel, R. Pohlner, O. Gühne and H. Weinfurter [31].

1. Fermionic qubits

The dimensionality of the accessible space for fermions, $\dim(\Xi_F)$, follows from mathematical properties of the determinant, since the coefficient $\tilde{g}_{j_1, \dots, j_N}$ in (30) can be expressed as the determinant of sub-matrices of W' .

We start with the case of qubits for simplicity, and re-write W' as a vector of $2N$, N -dimensional column vectors,

$$W' = (\vec{w}_1, \vec{w}_2, \dots, \vec{w}_{2N}). \quad (\text{B2})$$

With (30), we can write each coefficient of the state representation, $\tilde{g}_{j_1, \dots, j_N}$, as the determinant of the square matrix that consists of the respective columns of W' , *i.e.*

$$\tilde{g}_{j_1, \dots, j_N} = \text{Det}[(\vec{w}_{j_1}, \vec{w}_{2+j_2}, \dots, \vec{w}_{2N-2+j_N})]. \quad (\text{B3})$$

If W' does not have full rank (N), all coefficients $\tilde{g}_{j_1, \dots, j_N}$ vanish, because any set of N vectors w_{k_1}, \dots, w_{k_N} is then linearly dependent. We can thus assume that W' has full rank, and that the N vectors with odd index, $\vec{w}_1, \vec{w}_{2+1}, \dots, \vec{w}_{2(N-1)+1}$, are linearly independent. This assumption does not restrict generality, since simple re-shuffling of the matrix and re-labeling of degrees of freedom can always provide us with such a situation. Consequently, the remaining vectors with even indices ($\vec{w}_2, \vec{w}_4, \dots$) depend linearly on those with odd index, and we can always find coefficients $c_{2k}^{(2(j-1)+1)}$ such that

$$\forall k : \vec{w}_{2k} = \sum_{j=1}^N c_{2k}^{(2(j-1)+1)} \vec{w}_{2(j-1)+1}, \quad (\text{B4})$$

i.e. the vectors with even index can be expressed as linear combination of the vectors with odd index. In order to express (B3) in simpler terms, we use $\det(AB) = \det(A)\det(B)$, or, equivalently,

$$\begin{aligned} \text{Det} \left[\left(\sum_{j=1}^N b_j^{(1)} \vec{v}_j, \sum_{j=1}^N b_j^{(2)} \vec{v}_j, \dots, \sum_{j=1}^N b_j^{(N)} \vec{v}_j \right) \right] \\ = \text{Det} \left[\begin{pmatrix} b_1^{(1)} & b_2^{(1)} & \dots & b_N^{(1)} \\ \vdots & \vdots & \ddots & \vdots \\ b_1^{(N)} & b_2^{(N)} & \dots & b_N^{(N)} \end{pmatrix} \right] \\ \times \text{Det}[(\vec{v}_1, \vec{v}_2, \dots, \vec{v}_N)]. \quad (\text{B5}) \end{aligned}$$

In particular, the coefficient $\tilde{g}_{1,1,\dots,1}$ is given by the determinant of the matrix consisting of the odd vectors $\vec{w}_1, \vec{w}_3, \vec{w}_5 \dots \vec{w}_{2N-1}$ (see (30) and (B3)):

$$\tilde{g}_{1,1,\dots,1} = \text{Det}[(\vec{w}_1, \vec{w}_3, \dots, \vec{w}_{2N-1})] =: \mathcal{D}. \quad (\text{B6})$$

Since the vectors \vec{w}_{2k} depend linearly on the \vec{w}_{2l+1} , we can also express *all* other coefficients $\tilde{g}_{j_1, \dots, j_N}$ as a product of \mathcal{D} with determinants of matrices composed of the coefficients $c_l^{(m)}$. Therefore, *i.e.* exploiting (B5), we have

$$\begin{aligned} \tilde{g}_{1,1,\dots,1} &= \mathcal{D}, \\ \tilde{g}_{2,1,\dots,1} &= \mathcal{D} \cdot c_2^{(1)} = \mathcal{D} \cdot \text{Det} \left[\begin{pmatrix} c_2^{(1)} \end{pmatrix} \right], \\ &\vdots \\ \tilde{g}_{1,\dots,1,2} &= \mathcal{D} \cdot c_{2N}^{(2N-1)} = \mathcal{D} \cdot \text{Det} \left[\begin{pmatrix} c_{2N}^{(2N-1)} \end{pmatrix} \right], \\ \tilde{g}_{2,2,1,\dots,1} &= \mathcal{D} \cdot \left(c_2^{(1)} c_4^{(3)} - c_2^{(3)} c_4^{(1)} \right) \\ &= \mathcal{D} \cdot \text{Det} \left[\begin{pmatrix} c_2^{(1)} & c_2^{(3)} \\ c_4^{(1)} & c_4^{(3)} \end{pmatrix} \right], \\ &\vdots \\ \tilde{g}_{1,\dots,1,2,2} &= \mathcal{D} \cdot \left(c_{2N-2}^{(2N-3)} c_{2N}^{(2N-1)} - c_{2N-2}^{(2N-1)} c_{2N}^{(2N-3)} \right) \\ &= \mathcal{D} \cdot \text{Det} \left[\begin{pmatrix} c_{2N-2}^{(2N-3)} & c_{2N-2}^{(2N-1)} \\ c_{2N}^{(2N-3)} & c_{2N}^{(2N-1)} \end{pmatrix} \right]. \quad (\text{B7}) \end{aligned}$$

For a general systematic representation of the $\tilde{g}_{j_1, \dots, j_N}$ as they are given in (B7), we group the coefficients $c_{2k}^{(2(j-1)+1)}$ in a square $N \times N$ matrix \mathcal{C} with entries

$$\mathcal{C}_{k,j} = c_{2k}^{(2(j-1)+1)}, \quad (\text{B8})$$

such that the state coefficient $\tilde{g}_{j_1, \dots, j_N}$ is proportional to some *principle minor* (or *coaxial sub-determinant*) of \mathcal{C} [61], *i.e.* the determinant of the sub-matrix $\tilde{\mathcal{C}}(j_1, \dots, j_N)$ that is constructed as follows: For each k (with $1 \leq k \leq N$), delete the k th row and the k th column in the matrix \mathcal{C} if j_k is odd. The matrix $\tilde{\mathcal{C}}(j_1, \dots, j_N)$ is thus an $m \times m$ -submatrix of \mathcal{C} , and m is the number of even coefficients j_k , such that $0 \leq m \leq N$.

In particular, for $\tilde{g}_{1,1,1,\dots,1}$, all j_k are odd, and $\tilde{\mathcal{C}}(j_1, \dots, j_N)$ is the empty 0×0 matrix: All rows and columns have been deleted, and $\tilde{g}_{1,1,\dots,1} = \mathcal{D}$ – we set the determinant of the empty 0×0 -matrix to unity, for convenience. For $\tilde{g}_{2,2,2,\dots,2}$, one needs to compute the determinant of the full matrix $\mathcal{C} = \tilde{\mathcal{C}}(2, 2, \dots, 2)$, since all j_k are even. In general, we can rewrite the coefficients $\tilde{g}_{j_1, \dots, j_N}$ in the state expansion as a product of two determinants, just like in (B5):

$$\tilde{g}_{j_1, \dots, j_N} = \mathcal{D} \cdot \text{Det}[\tilde{\mathcal{C}}(j_1, \dots, j_N)]. \quad (\text{B9})$$

That is to say, the 2^N principle minors of \mathcal{C} (including the empty matrix and the full matrix) are the coefficients in the state representation. Since the values of $\vec{w}_1, \vec{w}_3, \dots, \vec{w}_{2N-1}$ only affect the determinant \mathcal{D} , they contribute to only one free parameter. Consequently, at this stage, the maximal number of independent parameters is bounded from above by $N^2 + 1$ (N^2 parameters for the matrix $\tilde{\mathcal{C}}$ and one parameter for \mathcal{D}).

Given the functional form of $\tilde{g}_{j_1, \dots, j_N}$ in terms of the principle minors of a matrix, we can actually find the exact number of independent parameters: The 2^N principle minors can be expressed by only $N^2 - N + 1$ parameters (a result which dates back to 1893 [92–94]). Consequently, we find

$$\dim(\Xi_F) = N^2 - N + 2. \quad (\text{B10})$$

The principle minors also allow us to find a minimal explicit parametrization for accessible fermionic states. Since the set of all N (1×1)-minors, all $(N(N-1)/2)$ (2×2)-minors and all $(N-1)(N-2)/2$ (3×3)-minors that include the first row and the first column are sufficient to span the set of all $2^N - 1$ minors [94], we can also express all accessible states in terms of these minors.

2. Fermionic qudits

In the case $d > 2$, we have a $(d \cdot N) \times N$ dimensional matrix W' that determines the scattering process. The vectors $\vec{w}_2, \dots, \vec{w}_d, \vec{w}_{d+2}, \dots, \vec{w}_{2d}, \dots, \vec{w}_{Nd}$ can be expressed as linear combination of the vectors $\vec{w}_1, \vec{w}_{d+1}, \dots, \vec{w}_{(N-1)d+1}$, such that, in analogy to (B4), we find

$$\forall k \neq 1 + d \cdot l : \vec{w}_k = \sum_{j=1}^N c_k^{(d(j-1)+1)} \vec{w}_{d(j-1)+1}, \quad (\text{B11})$$

and the $c_l^{(k)}$ fill a matrix of size $(d-1)N \times N$:

$$\mathcal{C} = \begin{pmatrix} c_2^{(1)} & c_2^{(d+1)} & c_2^{(2d+1)} & \dots & c_2^{((N-1)d+1)} \\ c_3^{(1)} & c_3^{(d+1)} & c_3^{(2d+1)} & \dots & c_3^{((N-1)d+1)} \\ \vdots & \vdots & \vdots & \ddots & \vdots \\ c_d^{(1)} & c_d^{(d+1)} & c_d^{(2d+1)} & \dots & c_d^{((N-1)d+1)} \\ c_{d+2}^{(1)} & c_{d+2}^{(d+1)} & c_{d+2}^{(2d+1)} & \dots & c_{d+2}^{((N-1)d+1)} \\ \vdots & \vdots & \vdots & \ddots & \vdots \\ c_{dN}^{(1)} & c_{dN}^{(d+1)} & c_{dN}^{(2d+1)} & \dots & c_{dN}^{((N-1)d+1)} \end{pmatrix} \quad (\text{B12})$$

In other words, for each additional dimension, we have to add N rows in the coefficient matrix. The d^N coefficients $\tilde{g}_{j_1, \dots, j_N}$ correspond to d^N minors of the matrix \mathcal{C} . Consequently, the accretion of one dimension leads to up to N^2 new parameters in the matrix \mathcal{C} and thus to at most N^2 new independent parameters. We thus have

$$\dim(\Xi_F) \leq (d-1)N^2 - N + 2, \quad (\text{B13})$$

which is the general bound for the dimensionality of the manifold of accessible states for N fermions with d internal states, when the fermions start in a non-entangled state.

3. Bosons

For bosons, the coefficients (30) are not the determinant of a sub-matrix of W' , but they instead correspond to the *permanent* [68–70]. Since the permanent of a product of two matrices is not necessarily the product of the permanents of the two matrices, the argument that allowed us to reduce the number of parameters for fermions immediately breaks down for bosons. Consequently, the lack of algebraic symmetry properties of the permanent leads to a larger value for the upper bound to the dimensionality of accessible states for bosons than for fermions.

In order to see this, we start with the dN^2 parameters $W'_{k,l}$ that govern the d^N coefficients g_{j_1, \dots, j_N} of the state. In the following, we identify $2N-1$ parameters that contribute to the normalization and to the global phase of the final state, and thus eliminate $2N-2$ of these.

Firstly, a complex factor that is applied to each group of d columns leads to a global factor in the final state. More precisely, a factor α_l to the l th group of d columns

corresponds to

$$W'_{j, (l-1) \cdot d + k} \rightarrow \alpha_l W'_{j, (l-1) \cdot d + k}, \quad (\text{B14})$$

for $1 \leq j \leq N$, $1 \leq l \leq N$, $1 \leq k \leq d$. By inserting the scaled W' into (30), we see that these factors lead to a global factor that only affects the normalization and the phase of the final state,

$$\tilde{g}_{j_1, \dots, j_N} \rightarrow \left(\prod_{l=1}^N \alpha_l \right) \tilde{g}_{j_1, \dots, j_N}. \quad (\text{B15})$$

In close analogy, the application of a factor to each row of W' , *i.e.*

$$W'_{j, (l-1) \cdot d + k} \rightarrow \beta_j W'_{j, (l-1) \cdot d + k}, \quad (\text{B16})$$

also gives a global factor

$$\tilde{g}_{j_1, \dots, j_N} \rightarrow \left(\prod_{l=1}^N \beta_l \right) \tilde{g}_{j_1, \dots, j_N}. \quad (\text{B17})$$

One of the N factors β_j can be absorbed by the α_k , such that the α_j and β_k only provide $2N-1$ independent parameters. In contrast to the determinant, there are no further symmetry properties that allow us to eliminate other parameters, which leads to the following bound for bosons:

$$\dim(\Xi_B) \leq dN^2 - 2N + 2, \quad (\text{B18})$$

which is always equal or higher than the corresponding bound for fermions, Eq. (B13).

-
- [1] J.-W. Pan, Z.-B. Chen, C.-Y. Lu, H. Weinfurter, A. Zeilinger, and M. Żukowski, *Rev. Mod. Phys.* **84**, 777 (2012).
 - [2] J. Bell, *Physics* **1**, 195 (1964).
 - [3] A. Aspect, P. Grangier, and G. Roger, *Phys. Rev. Lett.* **49**, 91 (1982).
 - [4] A. Aspect, P. Grangier, and G. Roger, *Phys. Rev. Lett.* **47**, 460 (1981).
 - [5] A. K. Ekert, *Phys. Rev. Lett.* **67**, 661 (1991).
 - [6] P. Walther, K. J. Resch, T. Rudolph, E. Schenck, H. Weinfurter, V. Vedral, M. Aspelmeyer, and A. Zeilinger, *Nature* **434**, 169 (2005).
 - [7] Y. H. Shih and C. O. Alley, *Phys. Rev. Lett.* **61**, 2921 (1988).
 - [8] D. Bouwmeester, J.-W. Pan, M. Daniell, H. Weinfurter, and A. Zeilinger, *Phys. Rev. Lett.* **82**, 1345 (1999).
 - [9] M. Eibl, S. Gaertner, M. Bourennane, C. Kurtsiefer, M. Żukowski, and H. Weinfurter, *Phys. Rev. Lett.* **90**, 220403 (2003).
 - [10] Z. Zhao, Y.-A. Chen, A.-N. Zhang, T. Yang, H. J. Briegel, and J.-W. Pan, *Nature* **430**, 54 (2004).
 - [11] C.-Y. Lu, X.-Q. Zhou, O. Gühne, W.-B. Gao, J. Zhang, Z.-S. Yuan, A. Goebel, T. Yang, and J.-W. Pan, *Nat. Phys.* **3**, 91 (2007).
 - [12] M. Rådmark, M. Żukowski, and M. Bourennane, *Phys. Rev. Lett.* **103**, 150501 (2009).
 - [13] R. Prevedel, G. Cronenberg, M. S. Tame, M. Paternostro, P. Walther, M. S. Kim, and A. Zeilinger, *Phys. Rev. Lett.* **103**, 020503 (2009).
 - [14] W. Wieczorek, R. Krischek, N. Kiesel, P. Michelberger, G. Tóth, and H. Weinfurter, *Phys. Rev. Lett.* **103**, 020504 (2009).
 - [15] X.-C. Yao, T.-X. Wang, P. Xu, H. Lu, G.-S. Pan, X.-H. Bao, C.-Z. Peng, C.-Y. Lu, Y.-A. Chen, and J.-W. Pan, *Nat. Photon.* **6**, 225 (2012).
 - [16] Y.-F. Huang, B.-H. Liu, L. Peng, Y.-H. Li, L. Li, C.-F. Li, and G.-C. Guo, *Nat. Commun.* **2**, 546 (2011).
 - [17] R. Horodecki, P. Horodecki, M. Horodecki, and K. Horodecki, *Rev. Mod. Phys.* **81**, 865 (2009).
 - [18] W. Wieczorek, N. Kiesel, C. Schmid, and H. Weinfurter, *Phys. Rev. A* **79**, 022311 (2009).
 - [19] R. Blatt and D. Wineland, *Nature* **453**, 1008 (2008).

- [20] S. Popescu, Phys. Rev. Lett. **99**, 130503 (2007).
- [21] J. Brendel, N. Gisin, W. Tittel, and H. Zbinden, Phys. Rev. Lett. **82**, 2594 (1999).
- [22] I. Marcikic, H. de Riedmatten, W. Tittel, H. Zbinden, M. Legré, and N. Gisin, Phys. Rev. Lett. **93**, 180502 (2004).
- [23] M. Halder, A. Beveratos, N. Gisin, V. Scarani, C. Simon, and H. Zbinden, Nat. Phys. **3**, 692 (2007).
- [24] M. N. O'Sullivan-Hale, I. Ali Khan, R. W. Boyd, and J. C. Howell, Phys. Rev. Lett. **94**, 220501 (2005).
- [25] A. Vaziri, G. Weihs, and A. Zeilinger, Phys. Rev. Lett. **89**, 240401 (2002).
- [26] R. Inoue, T. Yonehara, Y. Miyamoto, M. Koashi, and M. Kozuma, Phys. Rev. Lett. **103**, 110503 (2009).
- [27] A. Mair, A. Vaziri, G. Weihs, and A. Zeilinger, Nature **412**, 313 (2001).
- [28] L. Chen and W. She, Phys. Rev. A **83**, 012306 (2011).
- [29] R. T. Thew, A. Acín, H. Zbinden, and N. Gisin, Phys. Rev. Lett. **93**, 010503 (2004).
- [30] H. de Riedmatten, I. Marcikic, V. Scarani, W. Tittel, H. Zbinden, and N. Gisin, Phys. Rev. A **69**, 050304 (2004).
- [31] W. Wieczorek, C. Schmid, N. Kiesel, R. Pohlner, O. Gühne, and H. Weinfurter, Phys. Rev. Lett. **101**, 010503 (2008).
- [32] H. Hossein-Nejad, R. Stock, and D. F. V. James, Phys. Rev. A **80**, 022308 (2009).
- [33] C. Thiel, J. von Zanthier, T. Bastin, E. Solano, and G. S. Agarwal, Phys. Rev. Lett. **99**, 193602 (2007).
- [34] A. Maser, U. Schilling, T. Bastin, E. Solano, C. Thiel, and J. von Zanthier, Phys. Rev. A **79**, 033833 (2009).
- [35] U. Schilling, C. Thiel, E. Solano, T. Bastin, and J. von Zanthier, Phys. Rev. A **80**, 022312 (2009).
- [36] T. Bastin, C. Thiel, J. von Zanthier, L. Lamata, E. Solano, and G. S. Agarwal, Phys. Rev. Lett. **102**, 053601 (2009).
- [37] A. Maser, R. Wiegner, U. Schilling, C. Thiel, and J. von Zanthier, Phys. Rev. A **81**, 053842 (2010).
- [38] Y. L. Lim and A. Beige, Phys. Rev. A **71**, 062311 (2005).
- [39] N. Lütkenhaus, J. Calsamiglia, and K. A. Suominen, Phys. Rev. A **59**, 3295 (1999).
- [40] L. Vaidman and N. Yoran, Phys. Rev. A **59**, 116 (1999).
- [41] J. Calsamiglia, Phys. Rev. A **65**, 030301 (2002).
- [42] M. Huber, H. Schimpf, A. Gabriel, C. Spengler, D. Bruß, and B. C. Hiesmayr, Phys. Rev. A **83**, 022328 (2011).
- [43] T. Bastin, S. Krins, P. Mathonet, M. Godefroid, L. Lamata, and E. Solano, Phys. Rev. Lett. **103**, 070503 (2009).
- [44] B. Kraus, Phys. Rev. Lett. **104**, 020504 (2010).
- [45] B. Liu, J.-L. Li, X. Li, and C.-F. Qiao, Phys. Rev. Lett. **108**, 050501 (2011).
- [46] F. Mintert, B. Salwey, and A. Buchleitner, Many-body entanglement: Permutations and equivalence classes, arxiv:1109.6337.
- [47] P. Ribeiro and R. Mosseri, Phys. Rev. Lett. **106**, 180502 (2011).
- [48] M. C. Tichy, M. Tiersch, F. Mintert, and A. Buchleitner, N. J. Phys. **14**, 093015 (2012).
- [49] J. Eisert and H. J. Briegel, Phys. Rev. A **64**, 022306 (2001).
- [50] A. Halevy, E. Megidish, T. Shacham, L. Dovrat, and H. S. Eisenberg, Phys. Rev. Lett. **106**, 130502 (2011).
- [51] X. Zou and W. Mathis, Phys. Rev. A **71**, 042324 (2005).
- [52] S. Franke-Arnold, L. Allen, and M. Padgett, Laser & Photon. Rev. **2**, 299 (2008).
- [53] M. C. Tichy, F. Mintert, and A. Buchleitner, J. Phys. B **44**, 192001 (2011).
- [54] O. Gühne and G. Tóth, Phys. Rep. **474**, 1 (2009).
- [55] G. Ghirardi and L. Marinatto, Fortschr. Phys. **51**, 379 (2003).
- [56] G. Ghirardi and L. Marinatto, Phys. Rev. A **70**, 012109 (2004).
- [57] M. C. Tichy, F. de Melo, M. Kuś, F. Mintert, and A. Buchleitner, Fortschr. Phys. , doi:10.1002/prop.201200079 (2012).
- [58] M. A. Nielsen and I. L. Chuang, *Quantum computation and quantum information* (Cambridge University Press, Cambridge, 2000).
- [59] R. F. Werner, Phys. Rev. A **40**, 4277 (1989).
- [60] B. He, J. A. Bergou, and Z. Wang, Phys. Rev. A **76**, 042326 (2007).
- [61] D. S. Bernstein, *Matrix Mathematics* (Princeton University Press, Princeton, 2009).
- [62] X.-S. Ma, S. Kropatschek, W. Naylor, T. Scheidl, J. Kofler, T. Herbst, A. Zeilinger, and R. Ursin, Opt. Express **20**, 23126 (2012).
- [63] M. A. Nielsen, Phys. Rev. Lett. **83**, 436 (1999).
- [64] G. Vidal, J. Mod. Optic **47**, 355 (2000).
- [65] D. J. H. Markham, Phys. Rev. A **83**, 042332 (2011).
- [66] E. Majorana, Nuovo Cimento **9**, 43 (1932).
- [67] T. Sasaki, T. Ichikawa, and I. Tsutsui, Phys. Rev. A **83**, 012113 (2011).
- [68] H. J. Ryser, *Combinatorial Mathematics* The Carus mathematical monographs series (The Mathematical Association of America, 1963).
- [69] V. N. Sachkov and V. E. Tarakanov, *Combinatorics of Non-Negative Matrices* (American Mathematical Society, 2002).
- [70] S. Aaronson and A. Arkhipov, The computational complexity of linear optics, in *Proc. 43rd ACM Symp. Theo. Comp.*, STOC '11, p. 333, New York, NY, USA, 2011, ACM.
- [71] W. Wieczorek, *Multi-Photon Entanglement – Experimental Observation, Characterization, and Application of up to Six-Photon Entangled States*, PhD thesis, Ludwig-Maximilians-Universität München, 2009.
- [72] O. Benson, C. Santori, M. Pelton, and Y. Yamamoto, Phys. Rev. Lett. **84**, 2513 (2000).
- [73] C. Santori, D. Fattal, J. Vuckovic, G. S. Solomon, and Y. Yamamoto, Nature **419**, 594 (2002).
- [74] M. Förtsch, J. Fürst, C. Wittmann, D. Strekalov, A. Aiello, M. V. Chekhova, C. Silberhorn, G. Leuchs, and C. Marquard, A versatile source of single photons for quantum information processing, arxiv:1204.3056, 2012.
- [75] H. Lee, P. Kok, N. J. Cerf, and J. P. Dowling, Phys. Rev. A **65**, 030101 (2002).
- [76] G. J. Pryde and A. G. White, Phys. Rev. A **68**, 052315 (2003).
- [77] T. Brougham, V. Košťák, I. Jex, E. Andersson, and T. Kiss, Eur. Phys. J. D **61**, 231 (2011).
- [78] S.-Y. Baek and Y.-H. Kim, Phys. Rev. A **75**, 034309 (2007).
- [79] S.-Y. Baek, S. S. Straupe, A. P. Shurupov, S. P. Kulik, and Y.-H. Kim, Phys. Rev. A **78**, 042321 (2008).
- [80] B. P. Lanyon, T. J. Weinhold, N. K. Langford, J. L. O'Brien, K. J. Resch, A. Gilchrist, and A. G. White, Phys. Rev. Lett. **100**, 060504 (2008).
- [81] E. Megidish, T. Shacham, A. Halevy, L. Dovrat, and

- H. S. Eisenberg, Phys. Rev. Lett. **109**, 080504 (2012).
- [82] T. Peyronel, O. Firstenberg, Q.-Y. Liang, S. Hofferberth, A. V. Gorshkov, T. Pohl, M. D. Lukin, and V. Vuletic, Nature **488**, 57 (2012).
- [83] M. Hayashi, D. Markham, M. Murao, M. Owari, and S. Virmani, Phys. Rev. A **77**, 012104 (2008).
- [84] W. Dür, G. Vidal, and J. I. Cirac, Phys. Rev. A **62**, 062314 (2000).
- [85] C. Ammon, A. Maser, U. Schilling, T. Bastin, and J. von Zanthier, Simulating the coupling of angular momenta in distant matter qubits, arXiv:1207.4974, 2012.
- [86] M. Aulbach, D. Markham, and M. Murao, N. J. Phys. **12**, 073025 (2010).
- [87] P. Mathonet, S. Krins, M. Godefroid, L. Lamata, E. Solano, and T. Bastin, Phys. Rev. A **81**, 052315 (2010).
- [88] C.-Y. Lu, W.-B. Gao, O. Gühne, X.-Q. Zhou, Z.-B. Chen, and J.-W. Pan, Phys. Rev. Lett. **102**, 030502 (2009).
- [89] C.-Y. Lu, T. Yang, and J.-W. Pan, Phys. Rev. Lett. **103**, 020501 (2009).
- [90] J.-W. Pan and A. Zeilinger, Phys. Rev. A **57**, 2208 (1998).
- [91] F. Verstraete, J. Dehaene, B. De Moor, and H. Verschelde, Phys. Rev. A **65**, 052112 (2002).
- [92] P. A. MacMahon, Phil. Trans. R. Soc. Lond. A **185**, 111 (1893).
- [93] E. B. Stouffer, Trans. Am. Math. Soc. **26**, 356 (1924).
- [94] T. Muir, Phil. Mag. **38**, 537 (1894).